

Synthesis of Niobium Silicate Molecular Sieves of the MFI Structure: Evidence for Framework Incorporation of the Niobium Ion

A. M. Prakash and Larry Kevan*

Contribution from the Department of Chemistry, University of Houston, Houston, Texas 77204-5641

Received June 29, 1998

Abstract: A new electron spin resonance (ESR) method to identify incorporation of transition metals into the framework of zeolite molecular sieves is reported. A novel niobium silicate molecular sieve of MFI topology, designated here as NbS-1, is synthesized hydrothermally and characterized by ESR and other physical methods such as X-ray diffraction, thermogravimetric analysis, scanning electron microscopy, electron microprobe analysis, surface area measurements, and ^{29}Si MAS NMR, UV-visible, FTIR, and Raman spectroscopies. Substitution of niobium into the framework has been established by these various methods. γ -Irradiation of activated NbS-1 shows by ESR two radiation-induced hole centers (V centers) located on Si–O–Si and Nb–O–Si units of the framework. The latter can be identified through a 10-line hyperfine structure from ^{93}Nb ($I = 9/2$, 100% abundance) and provides convincing evidence for the incorporation of Nb into the silica framework. Nb(IV) ions are also formed as a consequence of radiation-induced reduction of Nb(V) associated with isolated tetrahedral NbO_4 units and exhibit an axially symmetric ESR signal with a 10-line hyperfine structure due to ^{93}Nb . Silicalite-1, on the other hand, shows radiation-induced hole centers located only on Si–O–Si units.

Introduction

Synthesis of transition metal containing molecular sieves (microporous as well as mesoporous) is one of the fastest developing areas in molecular sieve science due to the bifunctional characteristics of such materials in several catalytic reactions. Several transition metals have been substituted into crystalline silica or aluminophosphate frameworks to yield the corresponding metallosilicates or metalloaluminophosphate molecular sieves. Under controlled synthesis conditions, the metal can enter into the framework with the same coordination geometry as the parent element, which is tetrahedral coordination in these systems. Among the most widely known is the titanosilicate TS-1 originally discovered by Taramasso et al.¹ TS-1 is an excellent catalyst for the selective oxidation of various organic substrates in the presence of hydrogen peroxide.² Titanium substitution has been achieved in several other microporous and mesoporous silica molecular sieves to yield materials such as Ti- β , TS-2, TiZSM-48, TiMCM-41, and TiMCM-48. Other transition metals which are believed to be incorporated into crystalline silica frameworks are V, Fe, Mn, Co, Cr, etc., although the exact nature and coordination of these metals are still in debate.³ Also, synthesis methods have been developed to obtain transition metal substituted aluminophosphate molecular sieves.³ Examples in this class of materials are VAPO-5, CoAPO-5, TAPO-5, TAPO-11, etc. Recently, molecular sieves where transition metals enter into the framework in octahedral coordination were reported. ETS-10 and ETS-4 are examples in this class.^{4,5} Similarly, microporous and mesoporous molecular sieves composed of purely transition

metal oxide frameworks have been synthesized and characterized. Titania and niobia molecular sieves are examples in this class of materials.⁶ The metal coordination is found to be octahedral in these materials.

Niobium compounds have shown remarkable catalytic properties when they are used as components of catalysts or when small amounts are added to known catalysts. The effect of niobium oxide as a promoter, support, and solid acid has been studied in great detail.⁷ Niobium oxide as a single phase or in combination with other transition metal oxides has shown significant catalytic activity in a large number of reactions such as isomerization and oligomerization of olefins,⁸ oxidative dehydrogenation of alkane,⁹ alkylation of benzene,¹⁰ oxidation of methanol,¹¹ NO reduction by NH_3 ,⁷ and dehydration and dehydrogenation of alcohol.¹² Hydrated niobium pentoxide (niobic acid, $\text{Nb}_2\text{O}_5 \cdot n\text{H}_2\text{O}$) shows high acidity and catalytic activity for ethylene hydration¹³ and for the vapor phase esterification of ethyl alcohol.¹⁴ Photocatalytic activity of niobia mesoporous molecular sieves was reported recently.¹⁵ Niobium(V) monomers and dimers supported on SiO_2 are efficient catalysts for the dehydrogenation of ethanol.¹⁶ Substitution of niobium into silica frameworks of microporous materials has

(1) Taramasso, M.; Perego, G.; Notari, B. U.S. Patent 4 410 501, 1983.
 (2) Notari, B. *Adv. Catal.* **1996**, *41*, 253.
 (3) Szostak, R. *Molecular Sieves. Principles of Synthesis and Identification*; Van Nostrand Reinhold: New York, 1989; pp 205–281.
 (4) Kuznicki, S. M.; Thrush, K. A.; Allen, F. M.; Levine, S. M.; Hamil, M. M.; Hayhurst, D. T.; Mansour, M. In *Synthesis of Microporous Materials*; Occelli, M. L., Robson, H., Eds.; Van Nostrand Reinhold: New York, 1992; p 427.

(5) Anderson, M. W.; Terasaki, O.; Ohsuna, T.; Philippou, A.; MacKay, S. P.; Ferreira, A.; Rocha, J.; Lidin, S. *Nature* **1994**, *367*, 347.
 (6) (a) Sun, T.; Ying, J. Y. *Nature* **1997**, *389*, 704. (b) Antonelli, D. M.; Ying, J. Y. *Angew. Chem., Int. Ed. Engl.* **1996**, *35*, 426. (c) Antonelli, D. M.; Nakahira, A.; Ying, J. Y. *Inorg. Chem.* **1996**, *35*, 3126.
 (7) Tanabe, K. *Catal. Today* **1990**, *8*, 1.
 (8) Wada, Y.; Morikawa, A. *Catal. Today* **1990**, *8*, 13.
 (9) (a) Ruth, K.; Kieffer, R.; Burch, R. J. *Catal.* **1998**, *175*, 16. (b) Smits, R. H. H.; Seshan, K.; Leemreize, H.; Ross, J. R. H. *Catal. Today* **1993**, *16*, 513. (c) Ross, J. R. H.; Smits, R. H. H.; Seshan, K. *Catal. Today* **1993**, *16*, 503.
 (10) Okazaki, S.; Wada, N. *Catal. Today* **1993**, *16*, 349.
 (11) Jehng, J.-M.; Wachs, I. E. *Catal. Today* **1990**, *8*, 37.
 (12) Shirai, M.; Ichikuni, N.; Asakura, K.; Iwasawa, Y. *Catal. Today* **1990**, *8*, 57.
 (13) Ogasawara, K.; Iizuka, T.; Tanabe, K. *Chem. Lett.* **1984**, 645.
 (14) Chen, Z.; Iizuka, T.; Tanabe, K. *Chem. Lett.* **1984**, 108.
 (15) Stone, V. F., Jr.; Davis, R. J. *Chem. Mater.* **1998**, *10*, 1468.

not been attempted until recently when the synthesis of a titanium niobium silicate with the structure of nenadkevichite was reported.¹⁷ Titanium and niobium are suggested to be in distorted octahedral coordination in this material. As was reported for ETS-4 and ETS-10, these materials generally do not exhibit the catalytic properties typical of other titanosilicates in which Ti(IV) is in tetrahedral coordination.² However, such materials may find interesting catalytic applications after modifying them with other transition metals as reported recently for Pt- and Ru-modified ETS-10.¹⁸ The remarkable catalytic activity of TS-1 is attributed to coordinatively unsaturated Ti ions in a highly dispersed state. Our objective was therefore to prepare microporous materials in which niobium enters into tetrahedral coordination similar to the coordination of titanium in TS-1. We selected the MFI (silica) and AFI (aluminophosphate) structures as possible candidates for this purpose. In the present paper, we report results of our successful synthesis and characterization of niobium silicate molecular sieves of the MFI structure.

Identification of isomorphous substitution of transition metals in zeolite frameworks is a difficult problem. For many years, the idea that transition metals substitute for a tetrahedral framework site met with much criticism. On the basis of Pauling's ionic radii criterion and the lack of many transition metal tetrahedral oxides, many argued that such isomorphous substitution is unlikely. However, later work has shown that such substitution indeed takes place in several metallosilicate molecular sieves. Most of the attention has been focused on the titanosilicate TS-1, owing to its interesting catalytic properties. An array of characterization techniques have been employed to study the nature and location of Ti in a silica framework.^{2,19} Similar studies have been extended to other metallosilicate molecular sieves. Although, it is now generally accepted that titanium substitutes at a framework tetrahedral site in TS-1 and in other titanosilicates, conclusive evidence for framework metal substitution is still lacking for many other metallosilicates. In this paper, we report a new and efficient ESR method to identify framework incorporation of certain transition metals in zeolite molecular sieves.

Experimental Section

Synthesis. NbS-1 and silicalite-1 were prepared hydrothermally using tetrapropylammonium hydroxide as the organic template. The following chemicals were used without further purification: tetraethyl orthosilicate (98%, Aldrich), niobium ethoxide (99.95%, Aldrich), and tetrapropylammonium hydroxide (20 wt % in H₂O, TCI America). Doubly deionized water was used throughout. Syntheses were carried out in 100 cm³ stainless steel reactors lined with Teflon at autogenous pressure without agitation. On the basis of preliminary experiments, the following molar compositions were optimal for the synthesis of pure silicalite-1 and NbS-1 molecular sieves:



In a typical synthesis of NbS-1, 16 mL of (TPA)OH was added slowly to 14.17 g of tetraethyl orthosilicate with stirring. To about 10 mL of dry ethyl alcohol was added slowly with stirring 1.67 mL of

niobium ethoxide. The second solution was added dropwise to the silica solution. The mixture was stirred for 15 min. To this mixture was added slowly 6.36 mL of (TPA)OH mixed with 24 g of H₂O. The final solution was heated to about 340 K while being stirred. Water was added to compensate for the loss due to evaporation. The gel was light golden and transparent at this stage. The volume of the final gel was about 60 mL. The mixture was then transferred to an autoclave and heated to 443 K for 40 h without agitation. After crystallization, the product was separated from the mother liquor, washed with water, and dried at 353 K overnight. Two typical samples of NbS-1 with different niobium contents were synthesized. These samples are designated as NbS-1(0.05) and NbS-1(0.1), where the numbers in parentheses are the molar concentrations of NbO used in the initial synthesis gel.

According to the present route, our attempts to synthesize samples with higher niobium content were not successful as the final product was found to be mostly amorphous. The synthesis of silicalite-1 is same as above except that the step for the addition of Nb was omitted. A sample of TS-1 prepared according to the procedure reported²⁰ earlier was also used for the present investigation. The as-synthesized samples were calcined by raising the temperature slowly to 823 K in O₂ and then keeping the samples at this temperature for 16 h for removal of the organic template.

To check for possible occlusion of some niobia phase inside the channels of NbS-1, a calcined sample of NbS-1(0.1) was treated with 1 M ammonium acetate solution overnight and the solid was filtered off and washed several times with water. The surface area of this sample was then measured in comparison with that of the parent NbS-1 sample. Niobium(V) oxide (99.99%, Aldrich) was used as received. A physical mixture of niobium oxide and silicalite-1 was also prepared by thorough mixing of 5 wt % niobium oxide and 95 wt % calcined silicalite-1.

Sample Treatment and Measurements. Powder X-ray diffraction (XRD) patterns were recorded on a Siemens D5000 X-ray diffractometer using Cu K α radiation. The spectra were collected stepwise in the 4° ≤ 2θ ≤ 50° angular region, with 0.005° steps and 1 s counting time. Thermogravimetric (TG) analyses were carried out in O₂ on a 2050 TA Instrument at a heating rate of 10 K/min. Chemical analyses of the samples were carried out by electron probe microanalysis on a JEOL JXA-8600 spectrometer. The morphologies and particle sizes of the samples were studied by scanning electron microscopy. The surface areas of various samples were measured by using the multipoint BET method with N₂ physisorption at 77 K using a Micromeritics Gemini surface area analyzer. Electronic absorption spectra of calcined NbS-1 were recorded on a Perkin-Elmer 330 UV-visible spectrophotometer using silicalite-1 as a reference sample. ²⁹Si solid state MAS NMR spectra were obtained on a Unity 400 spectrometer using a zirconia rotor spun at a frequency of 9.2 kHz. The spectra were referenced against tetramethylsilane. FTIR spectra were measured on a Nicolet 740 FTIR spectrophotometer using KBr pellet techniques. Laser Raman spectra were obtained using a Spex 1403 double monochromator, equipped with 1800 groove/mm holographic gratings and a Hamamatsu 928 photomultiplier detection system under control of a Spex DM 3000 microcomputer system.²¹ The samples were excited by the 514.5 nm line of an Ar⁺ laser.

For ESR, samples of calcined NbS-1, calcined silicalite-1, bulk Nb₂O₅, and a Nb₂O₅-silicalite mixture were loaded into 3 mm o.d. × 2 mm i.d. Suprasil quartz tubes and the tubes were evacuated to a final pressure of 10⁻⁴ Torr at 295 K overnight. NbS-1 samples after calcination were normally exposed to atmospheric moisture before undertaking the ESR measurements. These samples contained significant amounts of water as measured by TG analysis. To study the behavior of the niobium as a function of hydration, NbS-1 samples were heated under vacuum from 295 to 673 K at regular intervals. For each interval, the temperature was raised slowly and that temperature was maintained for 16 h. Then ESR spectra were measured at 77 K to monitor any change in the sample by this treatment. To study the reduction behavior of NbS-1, samples were dehydrated at 673 K and then contacted with 1 atm of O₂ at 673 K for 16 h followed by

(16) (a) Nishimura, M.; Asakura, K.; Iwasawa, Y. *J. Chem. Soc., Chem. Commun.* **1986**, 1660. (b) Ichikuni, N.; Iwasawa, Y. *Catal. Today* **1993**, *16*, 427.

(17) Rocha, J.; Brandao, P.; Lin, Z.; Kharlanov, A.; Anderson, M. W. *J. Chem. Soc., Chem. Commun.* **1996**, 669

(18) (a) Das, T. K.; Chandwadkar, A. J.; Soni, H. S.; Sivasankar, S. *Catal. Lett.* **1997**, *44*, 113. (b) Bianchi, C. L.; Ragaini, V. *J. Catal.* **1997**, *168*, 70.

(19) Vayssilov, G. N. *Catal. Rev.—Sci. Eng.* **1997**, *39*, 209.

(20) Prakash, A. M.; Kevan, L. *J. Catal.* **1998**, *178*, 586.

(21) Czernuszewicz, R. S. In *Methods in Molecular Biology*; Jones, C., Mulloy, B., Thomas, A. H., Eds.; Humana Press: Totawa, NJ, 1993; Vol. 17, pp 345–374.

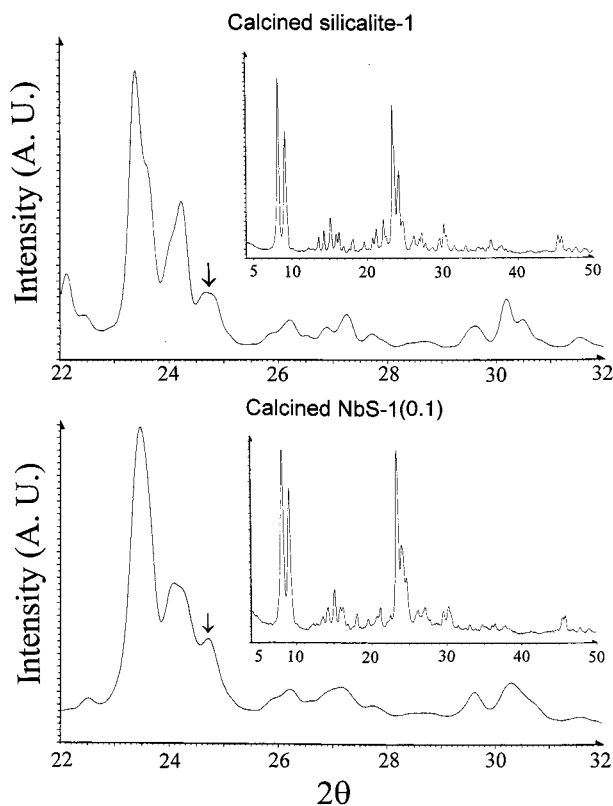


Figure 1. X-ray powder diffraction patterns of calcined silicalite-1 (top) and NbS-1(0.1) (bottom) molecular sieves in the region between 22 and 32°. The insets show the corresponding patterns in the region between 5 to 50°.

evacuation at the same temperature (activation). The activated samples were contacted with 350 Torr of dry hydrogen or 40 Torr of CO at 295 K and heated to various temperatures for varying durations before ESR measurements. In another reduction procedure, tubes containing activated samples were sealed and immersed in liquid nitrogen and then exposed to γ -irradiation from a ^{60}Co source at 77 K to a total dose of 4.4 Mrad at a dose rate of 0.18 Mrad h^{-1} . ESR spectra were recorded with a Bruker ESP 300 X-band spectrometer at 77 K. The magnetic field was calibrated with a Varian E-500 gaussmeter. The microwave frequency was measured by a Hewlett-Packard HP 5342A frequency counter.

Results and Discussion

Synthesis. In the synthesis of NbS-1, a pure MFI phase was obtained with a relatively low concentration of niobium (0.05–0.10 mol) in the synthesis gel. For higher niobium concentrations of 0.2 mol in the synthesis gel, the final product was found to be amorphous. Samples were characterized by X-ray powder diffraction. The observed patterns (Figure 1) confirm the MFI structure for both NbS-1 and silicalite-1. However, there are variations in the intensities of some lines between these two materials. A line at 22.2° observed for silicalite-1 is almost absent for NbS-1. Only a single line at 24.4° is observed for NbS-1 instead of a doublet observed for silicalite-1. A similar change has been observed for TS-1 molecular sieves in comparison to silicalite-1. Two reflections at 24.4 and 29.3° for TS-1 are split into doublets for silicalite-1. This is attributed to a change of symmetry from monoclinic to orthorhombic by the incorporation of titanium into the framework of silicalite. This is cited as strong evidence for the incorporation of Ti into the silicalite framework.²² The observed changes between NbS-1

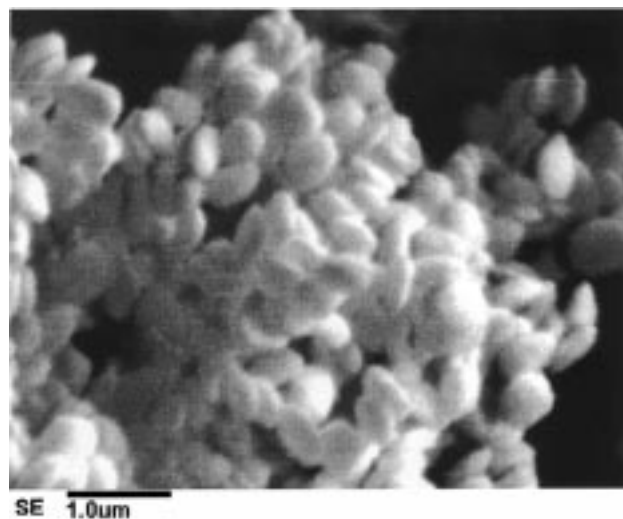
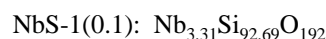
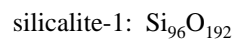


Figure 2. Electron micrograph of the NbS-1(0.1) molecular sieve. The scale bar is 1 μm .

and silicalite-1 also indicate the incorporation of Nb into the silicalite framework. Moreover, the observed XRD patterns do not show any peaks due to a crystalline Nb_2O_5 phase, thus excluding the possibility of any segregated crystalline niobia phase in our samples.

Both NbS-1 and silicalite-1 crystallize with particle sizes less than 1 μm according to the present synthesis route. A typical electron micrograph of NbS-1(0.1) is given in Figure 2. Elliptical morphology is observed for NbS-1. High crystallinity and phase purity are evident from these observations. The elemental analyses of the various samples were measured by electron microprobe analysis. The following compositions were obtained:



To investigate the thermal properties of the various MFI compositional variants, thermogravimetric analyses in flowing O_2 atmosphere of as-synthesized NbS-1 and silicalite-1 were carried out, and the results are shown in Figure 3. Both NbS-1(0.1) and NbS-1(0.05) show essentially the same weight loss curve. The initial small weight loss up to 400 K is due to the desorption of physically adsorbed water. The weight loss due to organic species takes place in multiple steps in both NbS-1 and silicalite-1. Three weight losses at 647, 669, and 694 K are observed in NbS-1. In silicalite-1, weight losses at 642, 657, 677, and 703 K are observed. These weight losses are probably due to the desorption and decomposition of the TPA species occluded inside the channels.²³ In both NbS-1(0.05) and NbS-1(0.1), the organic species accounted for 12.5 and 11.5%, respectively, of the total sample weight. In silicalite-1, this is about 13.5% of the total sample weight. These small but significant differences in the weight losses are possibly due to varying crystallinity of the individual samples. As the amount of niobium in the initial gel increases, the crystallinity of the final product decreases. We have observed a similar trend in the case of TS-1 and VS-1 molecular sieves. However, the observed weight losses in the present samples are comparable to or higher than the corresponding weight loss reported²³ for silicalite-1 which was synthesized in the presence of TPA. This

(22) Millini, R.; Massara, E. P.; Perego, G.; Bellussi, G. *J. Catal.* **1992**, *137*, 497.

(23) Franklin, K. R.; Lowe, B. M. *Zeolites* **1988**, *8*, 501.

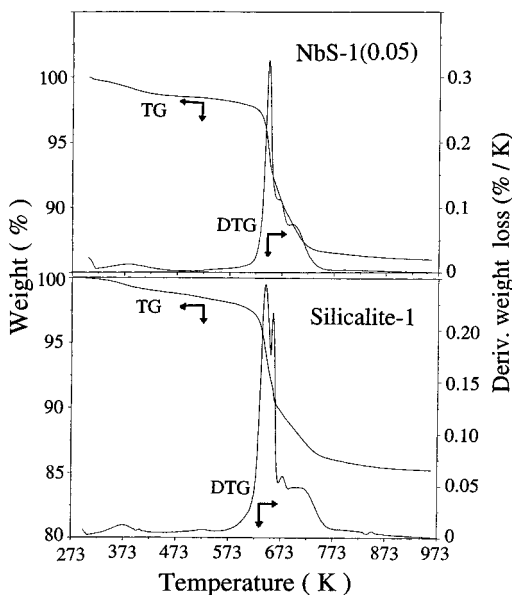


Figure 3. Thermogravimetric (TG) and differential thermogravimetric (DTG) curves of as-synthesized NbS-1(0.05) (top) and silicalite-1 (bottom) molecular sieves.

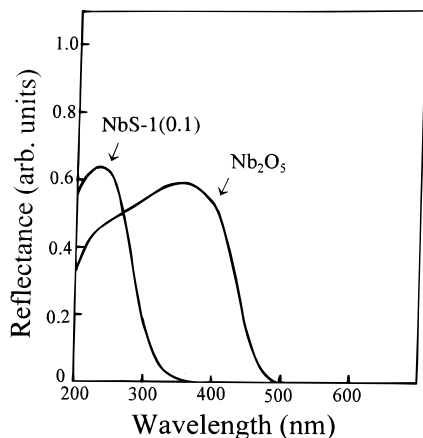


Figure 4. UV-visible diffuse reflectance spectra of calcined NbS-1(0.1) and bulk Nb₂O₅ materials. The spectra were obtained with silicalite-1 as a reference.

supports the high crystallinity of these samples. The NbS-1 structure is found to be stable up to 973 K, the maximum temperature investigated.

Various samples were analyzed for their surface areas. The BET surface areas obtained for NbS-1(0.05) and NbS-1(0.1) are 292 and 280 m²/g, respectively. After ammonium acetate treatment, NbS-1(0.1) shows a surface area of 286 m²/g, which is not significantly different from that of the parent sample. However, these values are somewhat lower than the surface area of silicalite-1 of 324 m²/g. The difference in the surface areas of NbS-1 and silicalite-1 is due either to low crystallinity or to occlusion of some Nb₂O₅ oxide phase inside the channels during synthesis. Since ammonium acetate treatment does not significantly change the surface area of NbS-1, the difference is more likely due to crystallinity. By the same reasoning, leaching of niobium from the framework during calcination is also excluded. This is further confirmed by electron microprobe analysis of NbS-1 after ammonium acetate treatment which shows the same Si/Nb ratio as before such treatment.

Figure 4 shows the diffuse reflectance ultraviolet-visible spectra of NbS-1(0.1) and Nb₂O₅. Both spectra were obtained with silicalite-1 as a reference. A transition with a maximum at

220 nm and absorption onset about 350 nm is observed for NbS-1(0.1). A similar but weak transition is observed for NbS-1(0.05). On the other hand, for niobia a very broad band with a maximum at 360 nm and an absorption onset near 500 nm is observed. Somewhat similar spectra have been reported for crystalline Nb₂O₅ and for mesoporous Nb₂O₅ materials.¹⁵ The same authors have also reported similar spectra for TiO₂ and mesoporous TiO₂. Diffuse reflectance UV-vis spectroscopy has been extensively used to probe the incorporation of Ti into tetrahedral framework sites of TS-1. The spectrum of TS-1 shows a strong transition at 210–220 nm attributed to a charge-transfer process localized on Ti(IV). This charge transfer occurs with electron excitation from the ligand oxygen to an unoccupied orbital of the central titanium ion and is therefore suggested to be associated with framework Ti(IV).¹⁹ The similar absorption spectra of NbS-1 and TS-1 suggest that the state of niobium in NbS-1 is similar to that of titanium in TS-1.

The observation of a broad UV absorption band in the spectrum of Nb₂O₅ is consistent with the known band gap of this material (410 nm). Anpo et al.²⁴ have proposed that the band energy gap position shifts to higher energy with a decrease in particle size of a semiconductor material. A sharp transition at 220 nm for NbS-1 therefore suggests that it is associated with local Nb–O bonds. Using diffuse reflectance and photoluminescence spectroscopy, Tanaka et al.²⁵ have studied highly dispersed niobia on a silica surface. For samples with low niobia loading, the diffuse reflectance spectra show a sharp absorption band between 200 and 330 nm with a maximum near 220 nm. In contrast, samples having high niobia loading show a broader absorption band between 200 and 370 nm with a maximum near 270 nm. On the basis of photoluminescence and X-ray absorption near edge structure results, the authors interpreted the band at 220 nm in the spectra of samples with low niobia loading as due to monomeric and oligomeric NbO₄ tetrahedra. A monomeric species is suggested in samples prepared by equilibrium adsorption, and oligomeric species are suggested in samples prepared by evaporation to dryness. The absorption band at 270 nm for samples with high niobia loading is assigned to microparticles of Nb₂O₅. The spectrum observed for NbS-1 is similar to those reported for samples with low niobia loading. Thus, we suggest that the band at 220 nm in the spectrum of NbS-1 is also due to NbO₄ tetrahedral units in this material.

Figure 5 shows the FTIR spectra of both NbS-1(0.1) and silicalite-1. Both spectra are similar except for a band at 971 cm⁻¹ in the former. A similar band has been observed for titanosilicates such as TS-1, TS-2, and Ti-β and also for other metallosilicates such as vanadium silicate, tin silicate, etc.^{19,26,27} The correct interpretation of this band is controversial. For titanosilicates, this band was initially assigned to surface titanyl species Ti=O or tetrahedral TiO₄ units. However, it is now generally accepted that the band at 960–970 cm⁻¹ is due to a Si–O vibrational mode perturbed by the presence of metal ions in a neighboring position and thus provides evidence for the incorporation of a metal ion into the framework.² Thus, we assign the band at 970 cm⁻¹ in the IR spectrum of NbS-1 to the presence of Si–O–Nb units in the framework. In the region of O–H stretching vibrations, only a broad band at 3440 cm⁻¹ is observed for both NbS-1 and silicalite-1. The intensity of

(24) Anpo, M.; Aikawa, N.; Kubokawa, Y.; Che, M.; Louis, C.; Giamello, E. *J. Phys. Chem.* **1985**, *89*, 5017.

(25) Tanaka, T.; Nojima, H.; Yoshida, H.; Nakagawa, H.; Funabiki, T.; Yoshida, S. *Catal. Today* **1993**, *16*, 297.

(26) Rao, P. R. H. P.; Ramaswamy, A. V.; Ratnasamy, P. *J. Catal.* **1992**, *137*, 225.

(27) Mal, N. K.; Ramaswamy, V.; Ganapathy, S.; Ramaswamy, A. V. *J. Chem. Soc., Chem. Commun.* **1994**, 1933.

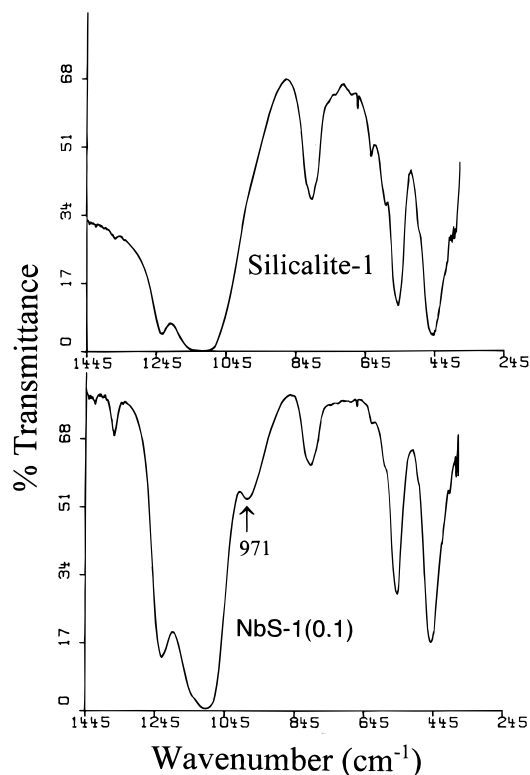


Figure 5. FTIR spectra of calcined silicalite-1 (top) and NbS-1 (0.1) (bottom) molecular sieves in the framework vibrational region.

this band is higher in the spectrum of NbS-1. A similar band has been observed for other metallosilicates and aluminosilicates and is assigned to surface silanol groups.¹⁹

Complementary to the IR observation, the Raman spectrum of NbS-1 shows two weak bands at 930 and 970 cm^{-1} , whereas these bands are absent in the spectrum of silicalite-1 (Figure 6). As with the IR assignment, these bands can be assigned to Nb–O–Si units of the framework. Niobium oxide structures in several niobium compounds have been studied by Raman spectroscopy.¹¹ Octahedrally coordinated NbO_6 with different extents of distortion due to corner- or edge-shared NbO_6 polyhedra is found in most niobium compounds. A few compounds such as YNbO_4 , LaNbO_4 , and SmNbO_4 have tetrahedrally coordinated NbO_4 . For tetrahedral NbO_4 , the major Raman band appears in the 790–830 cm^{-1} region. For distorted octahedral NbO_6 , the major Raman band appears in the 500–700 cm^{-1} region and also between 980 and 1000 cm^{-1} depending on the extent of distortion. It has been reported that the Raman spectrum of the titanium niobium silicate nenadkevichite exhibits two bands at 668 and 226 cm^{-1} which are assigned to NbO_6 octahedra.²⁸ Also Raman bands in the 600–800 cm^{-1} region assigned to NbO_6 have been reported for niobium silicate glasses.²⁹ These various bands are absent in the spectrum of NbS-1 and hence suggest the absence of any octahedral Nb in this material. It should be noted that in the 790–830 cm^{-1} region, where tetrahedral NbO_4 has its major Raman bands, both silicalite-1 and NbS-1 show bands at 802 and 833 cm^{-1} . Therefore, it is not immediately apparent from the Raman spectrum that NbO_4 units are present in NbS-1, although the bands in this region are slightly more intense for NbS-1 than for silicalite-1, which may suggest a possible additional contribution in the former.

(28) Rocha, J.; Brandao, P.; Lin, Z.; Esculcas, A. P.; Ferreira, A.; Anderson, M. W. *J. Phys. Chem.* **1996**, *100*, 14978.

(29) Fukumi, K.; Sakka, S. *J. Mater. Sci.* **1988**, *23*, 2819.

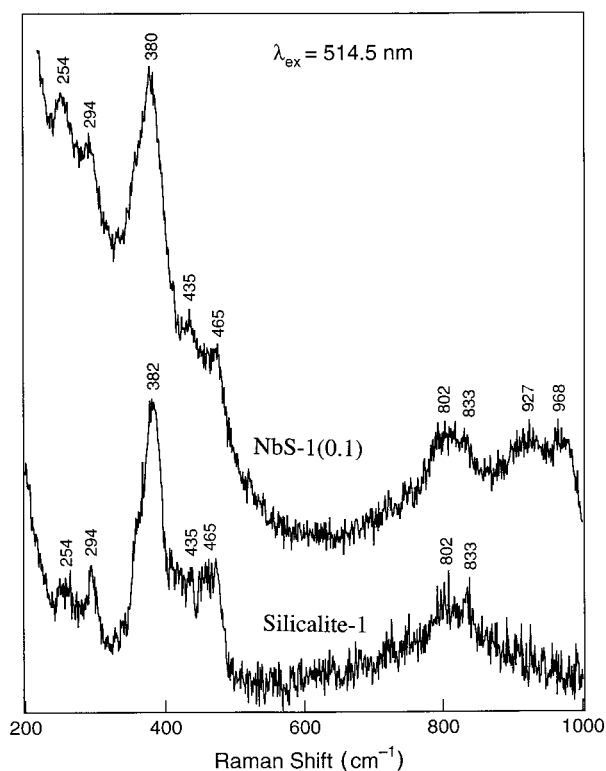


Figure 6. Laser Raman spectra of calcined NbS-1(0.1) and silicalite-1 molecular sieves.

Figure 7 shows the ^{29}Si MAS NMR spectra of NbS-1, silicalite-1, and TS-1. All spectra are essentially the same. A strong signal between –108 and –120 ppm centered at –113 ppm and another weak signal centered at –103 ppm are observed. The signal at –113 ppm is generally assigned as Si–(OSi)₄ units of the framework.³⁰ The width at half-maximum of this signal is slightly higher for NbS-1 and TS-1 than for silicalite-1. The small signal at –103 ppm is attributed to (HO)–Si(OSi)₃ units on the crystalline surface. This assignment was confirmed earlier by cross-polarization ^1H MAS NMR spectra in which the intensity of the signal at –103 ppm increased considerably with respect to the signal at –113 ppm.³¹ In an earlier study on TS-1, a shoulder at –115 to –116 ppm was also observed in the ^{29}Si MAS NMR spectrum.³² This signal was assigned to (TiO)Si(OSi)₃ units and cited as evidence for framework substitution of titanium. Since the observed signal in the spectrum of NbS-1 is broad enough to include any signal at –115 to –116 ppm, our MAS NMR measurement was not helpful in distinguishing the two environments of Si in Si(OSi)₄ and (NbO)Si(OSi)₃. For titanosilicate ETS-10, where titanium has octahedral coordination, multiple signals are observed between –94 and –105 ppm. These signals are assigned to Si–(OSi)₄ units and three crystallographically inequivalent (Ti_{oct}O)–Si(OSi)₃ units of the framework.⁵ If niobium in NbS-1 enters into the silica framework as octahedral, the observed NMR spectrum would have been different from that observed here. These observations together with the fact that the ^{29}Si NMR spectrum of NbS-1 is closely similar to that of TS-1 suggest that niobium in NbS-1 has 4-fold coordination. But unlike the

(30) Engelhardt, G. In *Introduction to Zeolite Science and Practice*; van Bekkum, H., Flanigen, E. M., Jansen, J. C., Eds.; *Studies in Surface Science and Catalysis*, Vol. 58; Elsevier: Amsterdam, 1991; Chapter 8, p 285.

(31) Huybrechts, D. R. C.; de Bruycker, L.; Jacobs, P. A. *J. Mol. Catal.* **1992**, *71*, 184.

(32) van der Pol, A. J. H. P.; Verduyn, A. J.; van Hooff, J. H. C. *Appl. Catal. A* **1992**, *92*, 113.

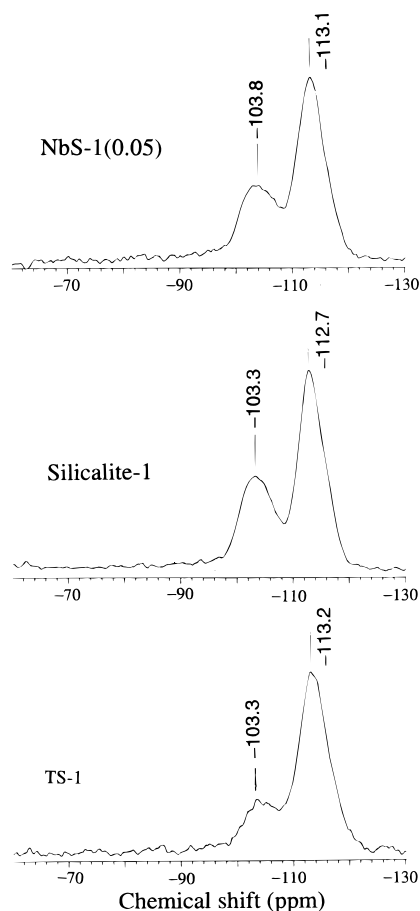


Figure 7. ^{29}Si MAS NMR spectra of calcined NbS-1(0.05) (top), silicalite-1 (middle), and TS-1 (bottom) molecular sieves.

case of TS-1, substitution of Nb(V) for Si(IV) generates an excess positive charge in the framework. This additional positive charge is probably balanced by hydroxyl groups or by non-framework anions. Because of the positive framework charge, NbS-1 is expected to have interesting applications as a basic catalyst.

The most convincing evidence for the substitution of Nb into the silicalite framework is obtained from ESR studies of activated NbS-1 samples after γ -irradiation. Calcined, dehydrated, and activated samples of NbS-1 and silicalite-1 show no ESR signal at 77 K. Under the same treatment conditions, pure Nb_2O_5 and Nb_2O_5 -silicalite mixture also do not show any signal. In addition, no signal is observed when NbS-1 is treated with H_2 or CO and subsequently heated to 673 K. We assume niobium in NbS-1 is nonparamagnetic Nb(V). Nb(IV) has a characteristic ESR spectrum as reported for γ -irradiated niobium silicate glass and other systems.³³⁻³⁵ The γ -irradiation of NbS-1 samples at 77 K induces a rich ESR spectrum with multiple signals. The observed ESR from γ -irradiated NbS-1 can be conveniently separated into two parts. One is the center-field spectrum shown in Figure 8; the other is the wide-field spectrum shown in Figure 9. As shown in Figure 8, the center-field spectrum of NbS-1 shows two strong superimposed signals A and B. Signal A has $g_{\text{av}} = 2.007$. Signal B has $g_{\text{av}} = 2.020$ and a 10-line hyperfine structure with a 0.0023 cm^{-1} splitting.

(33) Kim, Y. M.; Reardon, D. E.; Bray, P. J. *J. Chem. Phys.* **1968**, *48*, 3396.

(34) Stewart, C. P.; Porte, A. L. *J. Chem. Soc., Dalton Trans.* **1973**, *7*, 722.

(35) Fedotov, U. N.; Garifyanov, N. S.; Kozyrev, B. M. *Dokl. Akad. Nauk SSSR* **1962**, *145*, 1318.

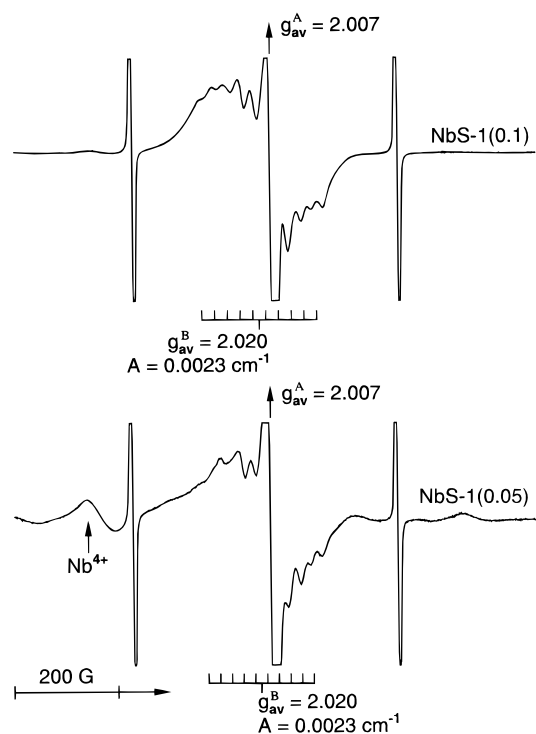


Figure 8. Central-field 77 K ESR spectra of activated NbS-1(0.1) (top) and NbS-1(0.05) (bottom) molecular sieves after γ -irradiation at 77 K.

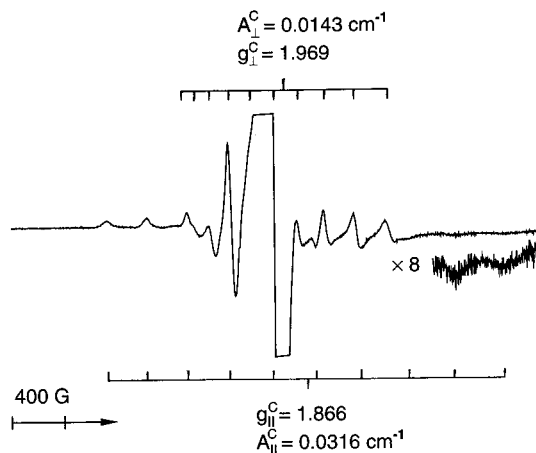


Figure 9. Wide-field 77 K ESR spectrum of the activated NbS-1(0.05) molecular sieve after γ -irradiation.

The center-field spectra observed for both NbS-1(0.05) and NbS-1(0.1) are essentially the same, although the hyperfine structure of signal B is more resolved for NbS-1(0.1). For comparison, Figure 10 shows the ESR spectra observed for silicalite-1 and a Nb_2O_5 -silicalite mixture. γ -Irradiated silicalite-1 shows a strong signal A with $g_{\text{av}} = 2.007$. A similar signal with somewhat lower intensity is observed for the Nb_2O_5 -silicalite mixture. Besides these signals, all samples show doublets separated by 505 G due to atomic hydrogen which disappear quickly at room temperature. The wide-field spectrum in Figure 9 is obtained for NbS-1(0.05) after γ -irradiation at 77 K for 24 h followed by annealing at room temperature for 10 s. The room-temperature annealing causes the hydrogen signal to decay. For NbS-1(0.1), the intensity of this signal is very low. We designate the wide-field signal as C. It should be mentioned that no ESR signal similar to A, B, or C is observed in the spectrum of pure Nb_2O_5 after γ -irradiation at 77 K.

The center-field spectrum (Figure 8) appears at approximately

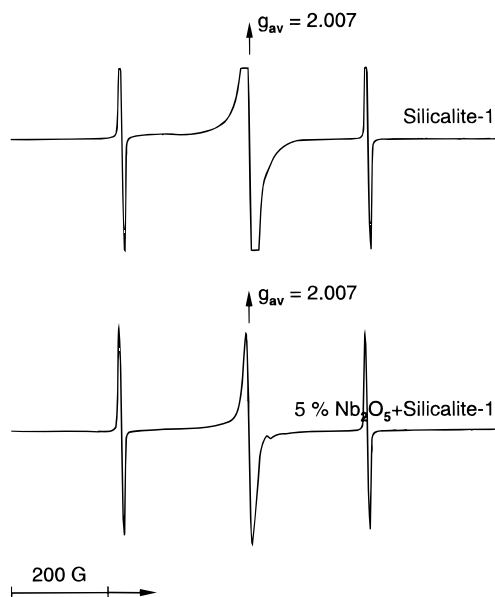


Figure 10. 77 K ESR spectra of activated silicalite-1 (top) and a Nb_2O_5 -silicalite (bottom) mixture after γ -irradiation.

the middle of the wide-field spectrum. Since the amplitude of the wide-field spectrum is comparatively small, its contribution to the center-field spectrum is not noticeable. This is especially true in the spectrum of NbS-1(0.1) where the intensity of C is low. Annealing experiments show that the center-field spectrum is a superposition of signals A and B. Signal A is observed for silicalite-1 and the Nb_2O_5 -silicalite mixture, whereas signal B is observed only for NbS-1 samples. The g values of signals A and B are greater than the free-electron g value of 2.0023. This indicates that these signals are for hole centers and not electron centers. The hyperfine coupling constant (0.0023 cm^{-1}) for signal B is considerably smaller than the coupling constant associated with signal C which is assigned to Nb(IV) (see below). Moreover, the measured g value for signal B is comparable to that of a hole center which is mainly localized on an oxygen in alkali metal silicate glasses and zeolite systems.^{36,37}

The effects of radiation on zeolites and other molecular sieves have been studied earlier. Several paramagnetic defect centers associated with the molecular sieve framework have been identified by ESR.^{37,38} In zeolites, both V_1 and V_2 centers associated with Al-O-Si and Si-O-Si units of the framework have been reported. These are radiation-induced hole centers trapped in the lone-pair p orbitals of the associated oxygen atoms. By incorporation of atoms with magnetic nuclei into the lattice, the nearby holes can be identified through hyperfine structure found in the ESR spectrum. In NbS-1, the only significantly abundant isotopic species having nonzero nuclear spin is ^{93}Nb ($I = 9/2$, 100% abundance). Signal A with $g_{\text{av}} = 2.007$ in the spectrum of NbS-1 is clearly due to defects generated on Si-O-Si units of the framework as the same signal is observed for silicalite-1. The second signal B with a 10-line hyperfine structure can clearly be assigned to hole centers located on Si-O-Nb units of the framework. Moreover, signal B cannot be assigned to defects generated on Nb-O-Nb units of any niobium oxides such as Nb_2O_5 which one might

possibly argue are present in extraframework locations. This is because no signal similar to B is observed for bulk Nb_2O_5 or for Nb_2O_5 -silicalite mixtures. Moreover, one expects more than 10 hyperfine lines for a defect located on a Nb-O-Nb unit due to the two Nb nuclei. Therefore, the presence of signal B with a 10-line hyperfine structure is strong evidence for the framework incorporation of niobium into NbS-1.

As shown in Figure 9, the wide-field spectrum is superposed on the center-field spectrum. Therefore, the central portion of the wide-field spectrum is not clearly resolved. Nevertheless, it can be seen from well-resolved shoulders that the spacing between consecutive resonance peaks increases with increasing magnetic field. The extent of this variation is shown by the separation of 301 G between the first two peaks on the low-field shoulder compared to the separation of 383 G between the final two peaks on the high-field side. This kind of unequal separation is observed in the ESR spectra of other transition metals such as V and Mn due to second-order hyperfine interactions.³⁹ Annealing and microwave power saturation experiments indicate that the wide-field spectrum arises from one ESR center. An ESR spectrum similar to signal C has been reported earlier for a niobium silicate Nb_2O_5 - Na_2O - SiO_2 glassy system after γ -irradiation.³³ The spectrum was interpreted as due to Nb(IV) centers generated on isolated NbO_6 units from reduction of Nb(V). The fact that signal C decreases in intensity significantly for NbS-1(0.1) is consistent with the observations made on niobium silicate glasses where this signal decreases in intensity with increasing niobium content. The observed ESR signal C is interpreted by the spin Hamiltonian given for a spin S in an axial field³³

$$H = g_{\parallel}H_zS_z + g_{\perp}(H_xS_x + H_yS_y) + A_{\parallel}S_zI_z + A_{\perp}(S_xI_x + S_yI_y) + P[I_z^2 - 1/3I(I+1)]$$

where $P = [3eQ(\partial^2V/\partial z^2)]/[4I(2I-1)]$; Q is the nuclear quadrupole moment, and $(\partial^2V/\partial z^2)$ is the zz component of the electric field gradient tensor at the nuclear site. According to an analysis similar to that for the niobium silicate glass system,³³ signal C has $g_{\perp} = 1.969$, $A_{\perp} = 0.0143 \text{ cm}^{-1}$, $g_{\parallel} = 1.866$, and $A_{\parallel} = 0.0316 \text{ cm}^{-1}$. The ESR parameters for the niobium glass system with niobium in octahedral coordination are $g_{\perp} = 1.921$, $A_{\perp} = 0.0164 \text{ cm}^{-1}$, $g_{\parallel} = 1.895$, and $A_{\parallel} = 0.0325 \text{ cm}^{-1}$. Signal C observed in the spectrum of NbS-1 cannot be assigned to any possible Nb_2O_5 nanophase which may be occluded inside the channels since similar species are not observed in bulk Nb_2O_5 or Nb_2O_5 -silicalite materials. On the basis of the ^{29}Si MAS NMR results, we have already eliminated the possibility of octahedral NbO_6 units present in the framework of NbS-1. Thus we assign signal C to Nb(IV) centers generated on NbO_4 tetrahedral units present in the framework of NbS-1. The observed difference in the ESR parameters between NbS-1 and niobium silicate glass can then be explained as a difference in coordination of Nb(IV) in these two materials.

A reaction mechanism which is consistent with the ESR results for both NbS-1 and silicalite-1 is given in Figure 11. Since the amount of niobium in NbS-1 is very small compared to that of silicon, one expects nearly the same intensity for signal A in the spectra of both silicalite and NbS-1. The proposed mechanism is consistent with the observation of signals B and C for NbS-1 samples. Niobium(V) in a Si-O-Nb unit can be reduced to Nb(IV) by γ -irradiation. However, it is still unclear why signal C has such a low intensity for NbS-1(0.1), where the Nb content is higher than that in NbS-1(0.05).

(36) Kim, Y. M.; Bray, P. J. *J. Chem. Phys.* **1970**, *53*, 716.

(37) (a) Abou-Kais, A.; Vedrine, J. C.; Massardier, J. *J. Chem. Soc., Faraday Trans.* **1975**, *71*, 1697. (b) Wichterlova, B.; Novakova, J.; Prasil, Z. *Zeolites* **1988**, *8*, 117.

(38) Hong, S. B.; Kim, S. J.; Uh, Y. S. *J. Am. Chem. Soc.* **1996**, *118*, 8102; *J. Phys. Chem.* **1996**, *100*, 15923.

(39) (a) Kivelson, D.; Lee, S.-K. *J. Chem. Phys.* **1964**, *41*, 1896. (b) Bleaney, B.; Ingram, D. J. E. *Proc. R. Soc. London* **1951**, *A205*, 336.

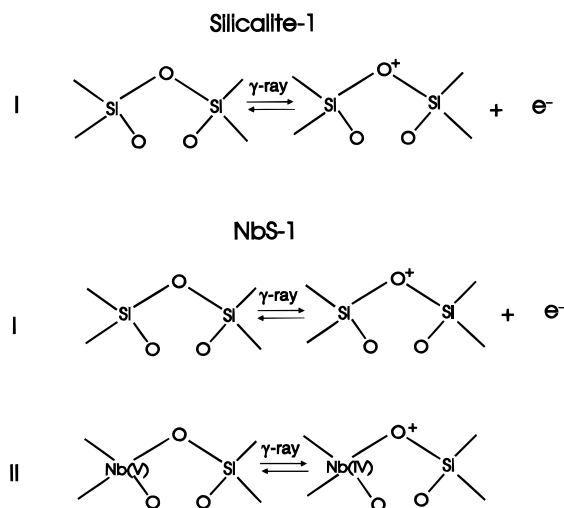


Figure 11. Reaction mechanisms for the formation of radiation-induced hole centers in silicalite-1 and NbS-1 molecular sieves.

Various characterization results for NbS-1 show that niobium has tetrahedral coordination in the calcined or dehydrated form. However, the possibility of niobium having higher coordination in as-synthesized or hydrated forms cannot be excluded. Our ESR measurements do not identify the coordination of niobium in as-synthesized NbS-1 since the spectra are dominated by a radical signal generated from an organic species.

It is interesting to compare the present observations with the ESR results for TS-1 and TiMCM-41 after γ -irradiation.^{20,40} When activated TS-1 or TiMCM-41 is γ -irradiated, the resultant ESR spectrum shows induced hole centers the same as signal A in the spectra of NbS-1 and silicalite-1 and also Ti(III) centers. Signal A for TS-1 or TiMCM-41 is higher in intensity than that for silicalite-1 or siliceous MCM-41. This correlates with the formation of Ti(III) centers in TS-1 and TiMCM-41. Unlike the case of NbS-1, for titanosilicate materials ESR spectra do not distinguish the hole centers generated on Si-O-Ti from those generated on Si-O-Si units. This is probably because of the low natural abundances of the ^{47}Ti ($I = 5/2$, natural

abundance 7.28%) and ^{49}Ti ($I = 7/2$, natural abundance = 5.51%) nuclei. Thus, the present method of identifying transition metals in the framework is limited to those metals having nonzero nuclear spins and high natural abundances. Metals such as vanadium (^{51}V , $I = 7/2$, 99.76%), manganese (^{55}Mn , $I = 5/2$, 100%), cobalt (^{59}Co , $I = 7/2$, 100%), and arsenic (^{75}As , $I = 3/2$, 100%) seem to be suitable candidates for this method. To check the validity of such a hypothesis, we recorded the ESR spectra of activated CoAPO-41 and AlPO-41 molecular sieves after γ -irradiation. As expected, the ESR spectrum of CoAPO-41 shows two characteristic signals which can be assigned to hole centers located on Co-O-P and Al-O-P units of the framework. AlPO-41, on the other hand, shows only a single signal due to hole centers located on Al-O-P units. The detailed analysis of this system will be a future subject.

Conclusions

Electron spin resonance spectroscopy offers a new method to identify the incorporation of certain transition metals into the framework of molecular sieves. A novel niobium silicate molecular sieve of MFI topology is synthesized hydrothermally and characterized by various physical methods. Substitution of niobium into the framework has been established. γ -Irradiation of an activated niobium silicate molecular sieve shows two radiation-induced hole centers (V centers) located on Si-O-Si and Nb-O-Si units of the framework. The latter is identified from a 10-line hyperfine structure from ^{93}Nb interaction and provides convincing evidence for the incorporation of Nb into the silica framework. Nb(IV) ions are also formed by radiolytic reduction of Nb(V) on isolated NbO_4 units and exhibit an axially symmetric ESR signal with a 10-line hyperfine structure. On the other hand, silicate-1 shows radiation induced hole centers located only on Si-O-Si units.

Acknowledgment. We thank Dr. M. Narayana for obtaining the ^{29}Si MAS NMR spectra and Prof. R. S. Czernuszewicz and Mr. D. Ji for performing the Raman measurements. This research was supported by the National Science Foundation and the Robert A. Welch Foundation.

(40) Prakash, A. M.; Sung-Suh, H M.; Kevan, L. *J. Phys. Chem. B* **1998**, *102*, 857.